Pulse Shaping in Unipolar OFDM-based Modulation Schemes

Dobroslav Tsonev, Sinan Sinanović and Harald Haas
Institute for Digital Communications, Joint Research Institute for Signal and Image Processing,
The University of Edinburgh, EH9 3JL, Edinburgh, UK
Email: {d.tsonev,s.sinanovic, h.haas}@ed.ac.uk

***Abstract*—This paper discusses the issue of pulse shaping in unipolar orthogonal-frequency-division-multiplexing-based modulation schemes for intensity modulation/direct detection systems. Three previously presented schemes, asymmetrically clipped optical OFDM, pulse-amplitude-modulated discrete multitone modulation, and unipolar orthogonal frequency division multiplexing, are investigated. The current work demonstrates how both unipolar and bipolar pulse shapes can be used for the generation of unipolar *continuous*-time signals.**

I. Introduction

Wireless data traffic is increasing exponentially [1]. Despite the continuous improvements in wireless communication technology, it is expected that the future demand cannot be met because the radio frequency spectrum has been almost completely utilised. A potential solution to the emerging problem is the development of optical wireless communication. Main advantages of an optical wireless system are: (a) a lot of unregulated bandwidth, (b) license-free operation, (c) low-cost front end devices, (d) no interference with the operation of sensitive electronic systems, (e) reuse of the existing lighting infrastructure, and (f) no health concerns related to visible light as long as eye-safety regulations are met [2].

The physical properties of light emitting diodes (LEDs) and photodiodes (PDs) characterise a visible light communication (VLC) system as an intensity modulation/direct detection (IM/DD) system. In other words, only signal intensity and no phase or amplitude can be conveyed. This fact limits the set of modulation schemes which can be employed. Techniques like on-off keying (OOK), pulse-position modulation (PPM), and pulse-amplitude modulation (PAM) can be applied in a straightforward fashion. With the increase of transmission rates, however, intersymbol interference (ISI) becomes an issue. Hence, a more resilient technique like orthogonal frequency division multiplexing (OFDM) becomes desirable. Conventional OFDM signals are complex and bipolar in nature. It is possible to generate real OFDM signals by imposing Hermitian symmetry on the carriers in frequency domain at the expense of half the spectral efficiency [2]. The bipolarity of signals, however, introduces an additional problem in VLC since LEDs can only be modulated with strictly positive signals. The issue can be solved by introducing a DC-bias, which increases the power dissipation of the system and cannot be easily optimised for all constellation sizes of quadrature amplitude modulation (M-QAM) used to modulate the different OFDM carriers. This technique is known as DC-biased optical OFDM (DCO-OFDM). Three power-efficient alternatives to DCO-OFDM have been proposed in previous works: asymmetrically clipped optical OFDM (ACO-OFDM) [3], pulse-amplitude-modulated discrete multitone modulation (PAM-DMT) [4], unipolar orthogonal frequency division multiplexing (U-OFDM) [5]. They use different properties of the OFDM frame for generation of unipolar signals, which do not require DC-biasing and achieve better power efficiency. To the best of our knowledge, all three techniques have been discussed in the context of *digital* signal processing without special consideration of the pulse shaping necessary for the generation of *continuous*-time bandlimited signals. The current work will focus on this issue and demonstrate that while special considerations need to be taken in the signal generation process, all the modulation concepts can be realised with commonly used pulse shapes. DCO-OFDM is not considered in this paper since it does not have the same issues because unipolarity is achieved through biasing in the analog domain.

The rest of this paper is organised as follows. Section II provides a description of the unipolar modulation schemes. Section III describes the problem which arises when bipolar pulses are used for the generation of a *continuous*-time signal and how it can be avoided. Section IV gives a theoretical justification to the solution proposed in Section III. Section V presents numerical results to confirm the theory. Finally, section VI gives concluding remarks.

II. Unipolar Modulation Schemes

A. ACO-OFDM

ACO-OFDM was introduced in [3]. In this scheme only odd subcarriers are modulated in frequency domain, which creates a certain symmetry in time domain. In general, if $s(k,n)$ is the contribution of subcarrier $S[k]$ to the sample at time n, then [3]

$$\begin{aligned} s(k,n) &= \frac{1}{\sqrt{N_{\text{fft}}}} S[k] e^{\frac{j2\pi nk}{N_{\text{fft}}}} \\ s(k,n+\frac{N_{\text{fft}}}{2}) &= \frac{1}{\sqrt{N_{\text{fft}}}} S[k] e^{\frac{j2\pi (n+N_{\text{fft}}/2)k}{N_{\text{fft}}}} = \\ &= \frac{1}{\sqrt{N_{\text{fft}}}} S[k] e^{\frac{j2\pi nk}{N_{\text{fft}}}} e^{j\pi k} \end{aligned} \quad (1)$$

If k is odd, $s(k,n) = -s(k,n+N_{\text{fft}}/2)$, and if k is even, $s(k,n) = s(k,n+N_{\text{fft}}/2)$. Then, if only the odd subcarriers in an OFDM frame are modulated, the time domain signal, $s[n]$, has the property

$$s[n] = -s[n+N_{\text{fft}}/2] \quad (2)$$

978-1-4673-4941-3/12/$31.00 ©2012 IEEE

If only the even subcarriers in an OFDM frame are modulated, the time-domain signal has the property

$$s[n] = s[n + N_{\text{fft}}/2] \tag{3}$$

Due to the orthogonality of the complex exponential functions, the property in (2) implies that only the odd subcarriers contain information, and the property in (3) implies that only the even subcarriers contain information. Clipping at zero of an arbitrary time-domain signal, $s[n]$, can be represented as

$$\text{CLIP}(s[n]) = \frac{1}{2}(s[n] + |s[n]|) \tag{4}$$

Because only the odd subcarriers are modulated in ACO-OFDM, equation (2) applies to the scheme. Therefore, $s[n] = -s[n+N_{\text{fft}}/2]$. Then $|s[n]| = |s[n+N_{\text{fft}}/2]|$. Hence, the clipping distortion $|s[n]|$, described in (4), possesses the property in (3) and falls on the even subcarriers only. The factor $\frac{1}{2}$ is consistent with the halving of the amplitudes, described in [3]. An additional factor of $\sqrt{2}$ should be used to preserve the amount of dissipated power, which would lead to an overall signal-to-noise ratio (SNR) penalty of 3dB. This simple proof is an alternative to the one presented in [3].

B. PAM-DMT

PAM-DMT was introduced in [4]. It modulates the carriers of an OFDM frame with symbols from the PAM modulation scheme, which are multiplied by $j = \sqrt{-1}$, and thus made imaginary. Due to the Hermitian symmetry in frequency domain of the OFDM frame, the PAM-DMT time-domain signal becomes [4]

$$\begin{aligned} s[n] &= \frac{1}{\sqrt{N_{\text{fft}}}} \sum_{k=0}^{N_{\text{fft}}-1} S[k] e^{\frac{j2\pi kn}{N_{\text{fft}}}} = \\ &= \frac{1}{\sqrt{N_{\text{fft}}}} \sum_{k=0}^{N_{\text{fft}}-1} S[k] \left(\cos \frac{2\pi kn}{N_{\text{fft}}} + j \sin \frac{2\pi kn}{N_{\text{fft}}} \right) = \\ &= \frac{1}{\sqrt{N_{\text{fft}}}} \sum_{k=0}^{N_{\text{fft}}-1} jS[k] \sin \frac{2\pi kn}{N_{\text{fft}}} \end{aligned} \tag{5}$$

The structure of PAM-DMT exhibits an antisymmetry where $s[0]{=}0$, $s[N_{\text{fft}}/2]{=}0$ if N_{fft} is even, and $s[n]{=}-s[N_{\text{fft}}-n]$. This means that $|s[0]|{=}0$, $|s[N_{\text{fft}}/2]|{=}0$ if N_{fft} is even, and $|s[n]|{=}|s[N_{\text{fft}}-n]|$. Therefore, after the clipping operation, described in (4), the distortion term $|s[n]|$ will possess Hermitian symmetry in time domain. This means that in frequency domain, the distortion will be translated into a real signal. Hence, it will be completely orthogonal to the original signal. The authors of [4] have not formally completed this proof. However, with the representation of clipping in (4), it is rather straightforward as presented here.

C. U-OFDM

U-OFDM was introduced in [5]. However, the authors in [6] present a very similar concept as Flip-OFDM. In the context of this work, the scheme will be referred to as U-OFDM. The idea is to separate a bipolar OFDM frame in two separate frames - positive and negative. The positive frame is a copy of the bipolar frame, where all negative values have been replaced with zeros. The negative frame is a copy of the bipolar frame where all samples are multiplied by -1, and again the negative ones are replaced with zeros. Therefore, the positive frame conveys the positive values in a unipolar positive signal, and the negative frame conveys the negative values in a unipolar positive signal. At the demodulator, they can be recombined by subtracting the negative frame from the positive one.

III. Pulse Shaping

Pulse shaping is used in communication systems for the generation of *continuous*-time signals that possess specific characteristics. A simple pulse shape is the Boxcar filter (a square pulse that corresponds to the zero-order hold function of a digital-to-analog converter (DAC)) [7]. It is easy to implement and simple to work with. However, it requires infinite bandwidth, which is very wasteful in wireless communications. The most spectrum efficient pulse shape is the sinc function $\text{sinc}(t) = \frac{\sin(\pi t)}{\pi t}$ [7]. However, it has a long impulse response, which is prone to ISI due to time jitter and is hard to realise. That is why, the raised-cosine filter and its modified version the root-raised-cosine filter present a more practical alternative. In addition, other pulse shapes like the hat function (a triangular pulse that corresponds to linear interpolation of samples) and the Gaussian filter exist. To the best of our knowledge, pulse shaping has not been considered for the schemes presented in Section II. It, however, is an integral part of any communication system and raises additional questions regarding the signal properties in the context of ACO-OFDM, PAM-DMT, and U-OFDM.

The three modulation approaches as presented in [3], [5], and [4] describe the process of generating a *discrete* unipolar signal. Discrete signals cannot be directly translated into *continuous* signals with the same properties if the bandwidth is limited. A *continuous*-time signal, $s(t)$, can be represented as a superposition of different copies of the pulse-shaping filter's impulse response, $p(t)$, scaled by the samples of the *discrete*-time signal, $s[n]$. It is presented in (6) where F indicates the frame order, $s[n, F]$ indicates the *discrete* signal $s[n]$ in frame F, N_{fft} indicates the number of fast Fourier transform (FFT) points in a single frame, N_{cp} indicates the length of the cyclic prefix, which is formed by the last N_{cp} points of $s[n, F]$. It is assumed that the phase is known, so $F{=}0$ corresponds to the current frame, and $t{=}0$ corresponds to the first sample position. If $p(t)$ is bipolar, and $s[n]$ is unipolar, $s(t)$ will tend to be bipolar as well. That is why, bipolar pulse shapes like the sinc function and the root-raised-cosine filter cannot be applied in a straightforward way to unipolar *discrete*-time signals. Unipolar shapes like the Boxcar filter, the hat function, and the Gaussian filter, can easily generate unipolar signals, but raise questions about how bandwidth efficient they are as well as how match filtering would be applied without generating intersymbol interference. The root-raised-cosine filter is a very practical pulse-shaping technique, which completely avoids ISI if there is no time jitter and provides an easy way to do match filtering. That is why, it will be used as the shaping pulse in the context of this paper. Fig. 1(a) illustrates the *continuous*-time signal generated by shaping a unipolar *discrete* ACO-OFDM signal with a root-raised-cosine filter. The result has negative values. This can be

$$s(t)=\sum_{F=-\infty}^{\infty}\left(\sum_{n=N_{\text{fft}}-N_{\text{cp}}}^{N_{\text{fft}}-1}s[n,F]p(t-F(N_{\text{fft}}+N_{\text{cp}})T_{\text{s}}-(n-N_{\text{fft}})T_{\text{s}})+\sum_{n=0}^{N_{\text{fft}}-1}s[n,F]p(t-F(N_{\text{fft}}+N_{\text{cp}})T_{\text{s}}-nT_{\text{s}})\right) \quad (6)$$

amended by introducing a DC-bias as in Fig. 1(b). However, it would increase the average power consumption approximately by 3dB, which would greatly reduce the power efficiency of the scheme. Alternatively, the negative values could be clipped, but this would lead to the distortion illustrated in Fig. 2(a). The other two schemes PAM-DMT and U-OFDM have exactly the same problem with a very similar performance degradation.

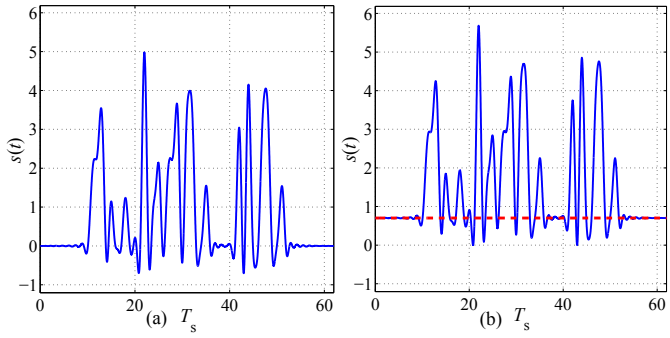

Fig. 1. (a) *Discrete* unipolar ACO-OFDM signal, shaped with a root-raised-cosine filter. (b) Signal from (a), biased to avoid clipping distortion.

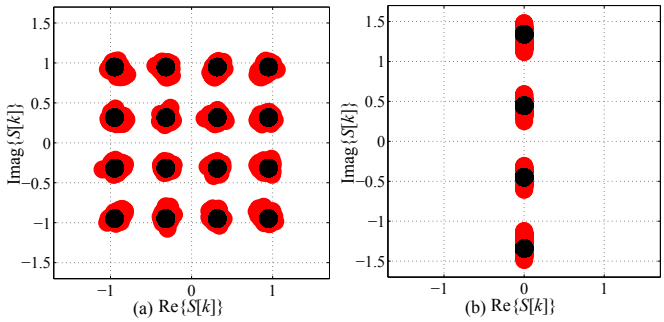

Fig. 2. (a) Distortion in the 16-QAM constellation after clipping negative values of the *continuous*-time signal. (b) Distortion in the 4-PAM constellation after clipping negative values of the *continuous*-time signal.

The rest of this paper will show that a bipolar pulse shape like the root-raised-cosine filter can be used without performance degradation in the previously described unipolar schemes if the *discrete*-time signal is kept bipolar and clipping is done after the pulse shaping operation. Fig. 3(a) illustrates a bipolar *discrete* ACO-OFDM signal shaped with a root-raised-cosine filter. Fig. 3(b) presents the signal, clipped after the pulse shaping operation. The next section shows analytically why the wave form from Fig. 3(b) retains the modulation concepts described in Section II, and distortion is avoided.

IV. Continuous-time Analysis

The complete *continuous*-time signal is presented in (6). Assume that the channel impulse response is causal, $h(t<0)=0$, and that the cyclic prefixes completely remove the ISI

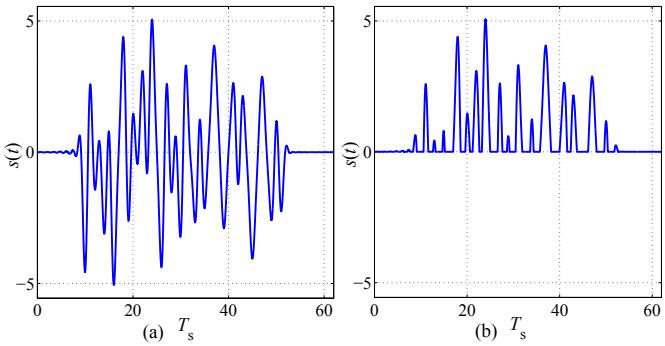

Fig. 3. (a) *Discrete* bipolar ACO-OFDM signal, shaped with a root-raised-cosine filter. (b) Signal from (a), made unipolar through clipping.

between the different OFDM frames. Hence, the portion of the *continuous*-time signal at the transmitter, which is relevant for sampling of the current frame, $F=0$, at the receiver, can be expressed as:

$$s(t)=\sum_{n=N_{\text{fft}}-N_{\text{cp}}}^{N_{\text{fft}}-1}s[n]p(t-(n-N_{\text{fft}})T_{\text{s}})+\sum_{n=0}^{N_{\text{fft}}-1}s[n]p(t-nT_{\text{s}})+ +\sum_{n=N_{\text{fft}}-N_{\text{cp}}}^{N_{\text{fft}}-N_{\text{cp}}+N_{\text{cp}}^{\text{P}}-1}s[n,1]p(t-(N_{\text{fft}}+N_{\text{cp}})T_{\text{s}}-(n-N_{\text{fft}})T_{\text{s}}) \quad (7)$$

where N_{cp}^{P} is the length of the cyclic prefix sufficient to remove the effects of $p(t)$, and $s[n]=s[n,0]$. The *continuous*-time signal relevant for sampling the first $\frac{N_{\text{fft}}}{2}$ points of the current frame can be expressed as

$$s_1(t)=\sum_{n=N_{\text{fft}}-N_{\text{cp}}}^{N_{\text{fft}}-1}s[n]p(t-(n-N_{\text{fft}})T_{\text{s}})+\sum_{n=0}^{N_{\text{fft}}/2-1}s[n]p(t-nT_{\text{s}})+ +\sum_{n=N_{\text{fft}}/2}^{N_{\text{fft}}/2-1+N_{\text{cp}}^{\text{P}}}s[n]p(t-nT_{\text{s}}) \quad (8)$$

The *continuous*-time signal relevant for sampling the second $\frac{N_{\text{fft}}}{2}$ points of the current frame can be expressed as

$$s_2(t)=\sum_{n=N_{\text{fft}}/2-N_{\text{cp}}}^{N_{\text{fft}}/2-1}s[n]p(t-nT_{\text{s}})+\sum_{n=N_{\text{fft}}/2}^{N_{\text{fft}}-1}s[n]p(t-nT_{\text{s}})+ +\sum_{n=N_{\text{fft}}-N_{\text{cp}}}^{N_{\text{fft}}-N_{\text{cp}}+N_{\text{cp}}^{\text{P}}-1}s[n,1]p(t-(N_{\text{fft}}+N_{\text{cp}})T_{\text{s}}-(n-N_{\text{fft}})T_{\text{s}}) \quad (9)$$

The *continuous*-time unipolar signal, ready for transmission, can be expressed as

$$s_{\text{c}}(t)=\sqrt{2}\text{CLIP}\left(s(t)\right)=\frac{1}{\sqrt{2}}\left(s(t)+|s(t)|\right) \quad (10)$$

Therefore, at the receiver, the samples of a given frame after match filtering can be expressed as

$$\hat{s}_{\rm h}[n] = (s_{\rm c}(t) * h(t) + n(t)) * p(t)|_{t=nT_{\rm s}} = \\ = \left(\frac{1}{\sqrt{2}}(s(t) + |s(t)|) * h(t) + n(t)\right) * p(t)\Big|_{t=nT_{\rm s}} = \\ = \begin{cases} \left(\frac{1}{\sqrt{2}}(s_1(t)+|s_1(t)|) * h(t)+n(t)\right) * p(t)\Big|_{t=nT_{\rm s}}, n \leq \frac{N_{\rm fft}}{2}-1 \\ \left(\frac{1}{\sqrt{2}}(s_2(t)+|s_2(t)|) * h(t)+n(t)\right) * p(t)\Big|_{t=nT_{\rm s}}, \frac{N_{\rm fft}}{2} \leq n \end{cases} \tag{11}$$

where $*$ denotes convolution and $n(t)$ denotes additive white Gaussian noise (AWGN). The cyclic prefix is sufficient to remove interference and to turn the *continuous*-time convolution with the channel, $h(t)$, into a circular convolution in *discrete* time, which can be completely reversed by equalisation. Hence, assuming the channel can be perfectly estimated, the equalised samples at the receiver can be expressed as

$$\hat{s}[n] = (s_{\rm c}(t) + n(t)) * p(t)|_{t=nT_{\rm s}} = \\ = \left(\frac{1}{\sqrt{2}}(s(t) + |s(t)|) + n(t)\right) * p(t)\Big|_{t=nT_{\rm s}} = \\ = \begin{cases} \left(\frac{1}{\sqrt{2}}(s_1(t)+|s_1(t)|) + n(t)\right) * p(t)\Big|_{t=nT_{\rm s}}, n \leq \frac{N_{\rm fft}}{2}-1 \\ \left(\frac{1}{\sqrt{2}}(s_2(t)+|s_2(t)|) + n(t)\right) * p(t)\Big|_{t=nT_{\rm s}}, \frac{N_{\rm fft}}{2} \leq n \end{cases} \tag{12}$$

A. ACO-OFDM

From the properties of ACO-OFDM, $s[n] = -s[n+N_{\rm fft}/2]$. Hence, in this scheme $s_1(t) \approx -s_2(t + \frac{N_{\rm fft}}{2}T_{\rm s})$ except for the third terms in (8) and (9). The differences appear due to the noncausal nature of $p(t)$ but are not significant when $N_{\rm cp}^{\rm p} << N_{\rm fft}$. This also implies $|s_1(t)| \approx |s_2(t + \frac{N_{\rm fft}}{2}T_{\rm s})|$. At the receiver, the distortion term in the first $\frac{N_{\rm fft}}{2}$ points, $\frac{1}{\sqrt{2}}|s_1(t)| * h(t) * p(t)\Big|_{nT{\rm s}}$, is the same as the distortion term in the second $\frac{N_{\rm fft}}{2}$ points, $\frac{1}{\sqrt{2}}|s_2(t)| * h(t) * p(t)\Big|_{nT{\rm s}}$, because $|s_1(t)| \approx \left|s_2\left(t + \frac{N_{\rm fft}}{2}T_{\rm s}\right)\right|$. Hence, distortion will fall on the even subcarriers as in (3).

B. PAM-DMT

From the properties of PAM-DMT, $s[n] = -s[N_{\rm fft} - n]$. Hence, using the representations in (8) and (9), $s_1(t) \approx -s_2(N_{\rm fft}T_{\rm s} - t)$. Differences are observed between the first term in (8) and the third term in (9) as well as between a single point in the third term of (8) and a single point in the first term of (9). The differences appear due to the noncausal nature of $p(t)$ but are not significant for $N_{\rm cp}^{\rm p} << N_{\rm fft}$. This also implies $|s_1(t)| \approx |s_2(N_{\rm fft}T_{\rm s} - t)|$. The impulse response of the pulse-shaping filter is even. Therefore, $p(t) = p(-t)$. Hence, a closer look at equation (12) shows that the distortion term after equalisation, formed by $\frac{1}{\sqrt{2}}|s_1(t)| * p(t)\Big|_{t=nT_{\rm s}}$ and $\frac{1}{\sqrt{2}}|s_2(t)| * p(t)\Big|_{t=nT_{\rm s}}$, keeps its Hermitian symmetry, and so it is orthogonal to the useful information as described in Section II-B.

C. U-OFDM

The U-OFDM bipolar *discrete* signal is encoded in two consecutive frames. The *continuous*-time bipolar part of $s(t)$ which needs to be sampled for the positive frame can be expressed before transmission as $s_{\rm up}(t)$ in the form of equation (7). The *continuous*-time bipolar part of $s(t)$ which holds the information of the negative frame can be expressed in the same form as $s_{\rm un}(t)$. If $s_{\rm up}[n]$ are the original bipolar samples of the positive frame, and $s_{\rm un}[n]$ are the original bipolar samples of the negative frame, then by design $s_{\rm up}[n] = -s_{\rm un}[n]$. Hence, a closer look at equation (7) shows that $s_{\rm up}(t) = -s_{\rm un}(t)$ except for the third terms in the summation. The differences appear due to the noncausal nature of $p(t)$ but are not significant when $N_{\rm cp}^{\rm p} << N_{\rm fft}$. Then, after match filtering at the receiver, the samples of the positive frame and the samples of the negative frame become respectively

$$\hat{s}_{\rm hup}[n] = \left(\frac{1}{2}(s_{\rm up}(t) + |s_{\rm up}(t)|) * h(t) + n_1(t)\right) * p(t)\Big|_{t=nT_{\rm s}} \tag{13}$$

$$\hat{s}_{\rm hun}[n] = \left(\frac{1}{2}(s_{\rm un}(t) + |s_{\rm un}(t)|) * h(t) + n_2(t)\right) * p(t)\Big|_{t=nT_{\rm s}} \tag{14}$$

where $n_1(t)$ and $n_2(t)$ are two independent identically-distributed instances of the AWGN process. The bipolar samples at the receiver can be reconstructed by subtracting the samples of the negative frame from the samples of the positive frame

$$\hat{s}_{\rm hb}[n] = \hat{s}_{\rm hup}[n] - \hat{s}_{\rm hun}[n] = \\ = \left(\frac{1}{2}(s_{\rm up}(t) - s_{\rm un}(t)) * h(t) + n_1(t) - n_2(t)\right) * p(t)\Big|_{t=nT_{\rm s}} \tag{15}$$

The nonlinear distortion terms $\frac{1}{2}|s_{\rm up}(t)| * h(t) * p(t)\Big|_{t=nT_{\rm s}}$ and $\frac{1}{2}|s_{\rm un}(t)| * h(t) * p(t)\Big|_{t=nT_{\rm s}}$ are equal and so are completely removed by the subtraction operation. The noise doubles as shown in [5] and [6].

For all three schemes, a cyclic suffix with length $N_{\rm cp}^{\rm p}$ could be added at the end of each frame to counter the effect of subsequent frames and remove the ISI and resulting distortion due to the noncausal impulse response of the pulse-shaping filter. The value of $N_{\rm cp}^{\rm p}$ depends on $p(t)$.

V. Numerical Results

Monte Carlo simulations with 16-QAM ACO-OFDM, 16-QAM U-OFDM, and 4-PAM PAM-DMT have been conducted in order to confirm the theory from Section IV. Figs. 4(a)-4(c) present the results for $N_{\rm fft}$=64 and a cyclic prefix with length $N_{\rm cp}$=5. The channel has been assumed flat with gain 1. As can be observed from the examples, the original signal is almost completely recovered if clipping is done after the pulse shaping. Nevertheless, some distortion is still present due to the noncausal impulse response of the shaping filter. Figs. 4(d)-4(f) present the results for $N_{\rm fft}$=64 and the addition of a cyclic suffix with length $N_{\rm cp}^{\rm p}$=5. The cyclic suffix improves

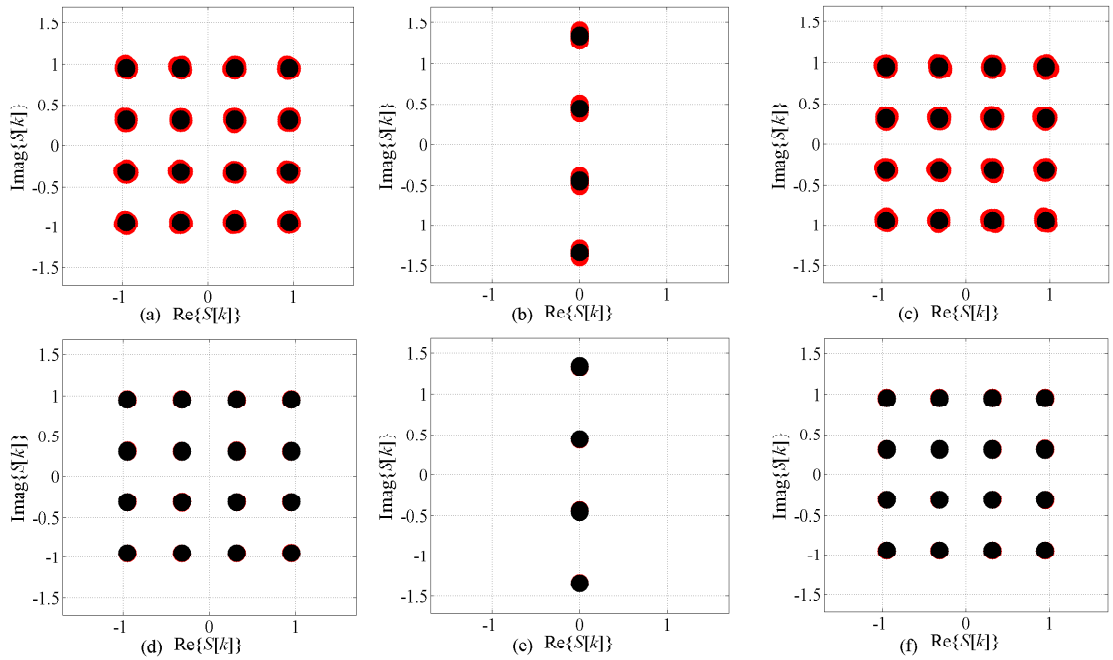

Fig. 4. (a) 16-QAM ACO-OFDM with a prefix only. (b) 4-PAM PAM-DMT with a prefix only. (c) 16-QAM U-OFDM with a prefix only. (d) 16-QAM ACO-OFDM with a prefix and a suffix. (e) 4-PAM PAM-DMT with a prefix and a suffix. (f) 16-QAM U-OFDM with a prefix and a suffix.

TABLE I
SDR VALUES FOR 16-QAM ACO-OFDM, 16-QAM U-OFDM, AND 4-PAM PAM-DMT FOR DIFFERENT NUMBER OF FRAME CARRIERS

N_{fft}	ACO-OFDM SDR [dB]		PAM-DMT SDR [dB]		U-OFDM SDR [dB]	
	Prefix Only	Prefix & Suffix	Prefix Only	Prefix & Suffix	Prefix Only	Prefix & Suffix
16	35.43	58.06	37.17	60.35	36.69	57.77
64	41.18	63.48	42.88	65.33	42.92	62.88
256	47.16	67.65	48.21	69.19	47.96	67.66

the recovered signal as expected. We define signal-to-distortion ratio (SDR) as

$$\text{SDR} = \frac{\text{E}\left[S^2[k]\right]}{\text{E}\left[\left(S[k] - \bar{S}[k]\right)^2\right]} \tag{16}$$

where $\bar{S}[k]$ denotes the distorted carrier values after pulse shaping and clipping, $\text{E}[\cdot]$ denotes expectation. Table I shows the SDR for a varying number of carriers, N_{fft}. It also shows the SDR for cases with and without a suffix. Increasing the number of carriers improves the SDR as the influence of subsequent frames becomes a smaller part of the overall signal. Adding a cyclic suffix improves the SDR significantly as it removes a big portion of the ISI caused by the pulse-shaping filter.

VI. Conclusion

Pulse shaping is an integral part of a communication system. Pulse shaping filters differ in terms of bandwidth requirements, ISI, and polarity. *Discrete* unipolar signals require unipolar pulse shapes to avoid bipolarity without additional power dissipation. If pulse shaping is applied before clipping, bipolar pulse-shaping filters can be used for the three modulation schemes ACO-OFDM, U-OFDM, and PAM-DMT, and in-band interference can be avoided. The structure of the interference terms suggests that even out-of-band interference could be avoided between systems that employ the same modulation concept. This could be a subject of further investigation.

Acknowledgement

We gratefully acknowledge support for this work from the UK Engineering and Physical Sciences Research Council (EPSRC) under grant EP/I013539/1.

References

[1] "Visible Light Communication (VLC) - A Potential Solution to the Global Wireless Spectrum Shortage," GBI Research, Tech. Rep., 2011. [Online]. Available: http://www.gbiresearch.com/

[2] H. Elgala, R. Mesleh, and H. Haas, "Indoor Optical Wireless Communication: Potential and State-of-the-Art," *IEEE Commun. Mag.*, vol. 49, no. 9, pp. 56–62, Sep. 2011, ISSN: 0163-6804.

[3] J. Armstrong and A. Lowery, "Power Efficient Optical OFDM," *Electronics Letters*, vol. 42, no. 6, pp. 370–372, Mar. 16, 2006.

[4] S. C. J. Lee, S. Randel, F. Breyer, and A. M. J. Koonen, "PAM-DMT for Intensity-Modulated and Direct-Detection Optical Communication Systems," *IEEE Photonics Technology Letters*, vol. 21, no. 23, pp. 1749–1751, Dec. 2009.

[5] D. Tsonev, S. Sinanović, and H. Haas, "Novel Unipolar Orthogonal Frequency Division Multiplexing (U-OFDM) for Optical Wireless," in *Proc. of the Vehicular Technology Conference (VTC Spring)*, IEEE. Yokohama, Japan: IEEE, May 6–9 2012, to appear.

[6] N. Fernando, Y. Hong, and E. Viterbo, "Flip-OFDM for Optical Wireless Communications," in *Information Theory Workshop (ITW)*, IEEE. Paraty, Brazil: IEEE, Oct., 16–20 2011, pp. 5–9.

[7] J. G. Proakis and D. K. Manolakis, *Digital Signal Processing: Principles, Algorithms and Application*, 4th ed., T. Robbins, Ed. Prentice Hall, Apr. 2006.